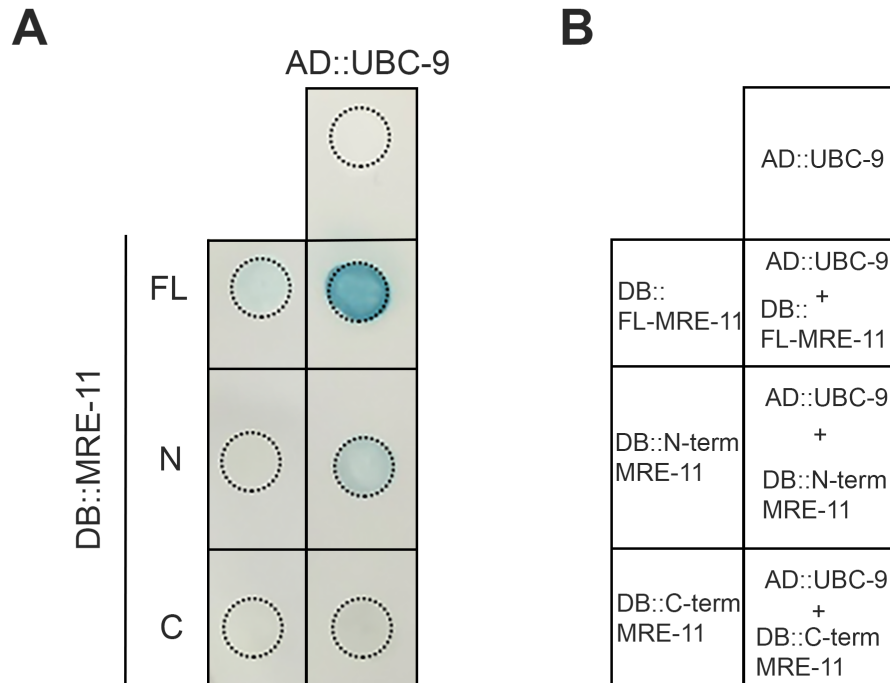


**Mitotic and meiotic functions for the SUMOylation pathway in the *Caenorhabditis elegans*
germline**

Reichman Rachel*, Shi Zhuoyue*, Malone Robert* and Smolikove Sarit*[†]

Supplementary figures 1-5

Figure S1



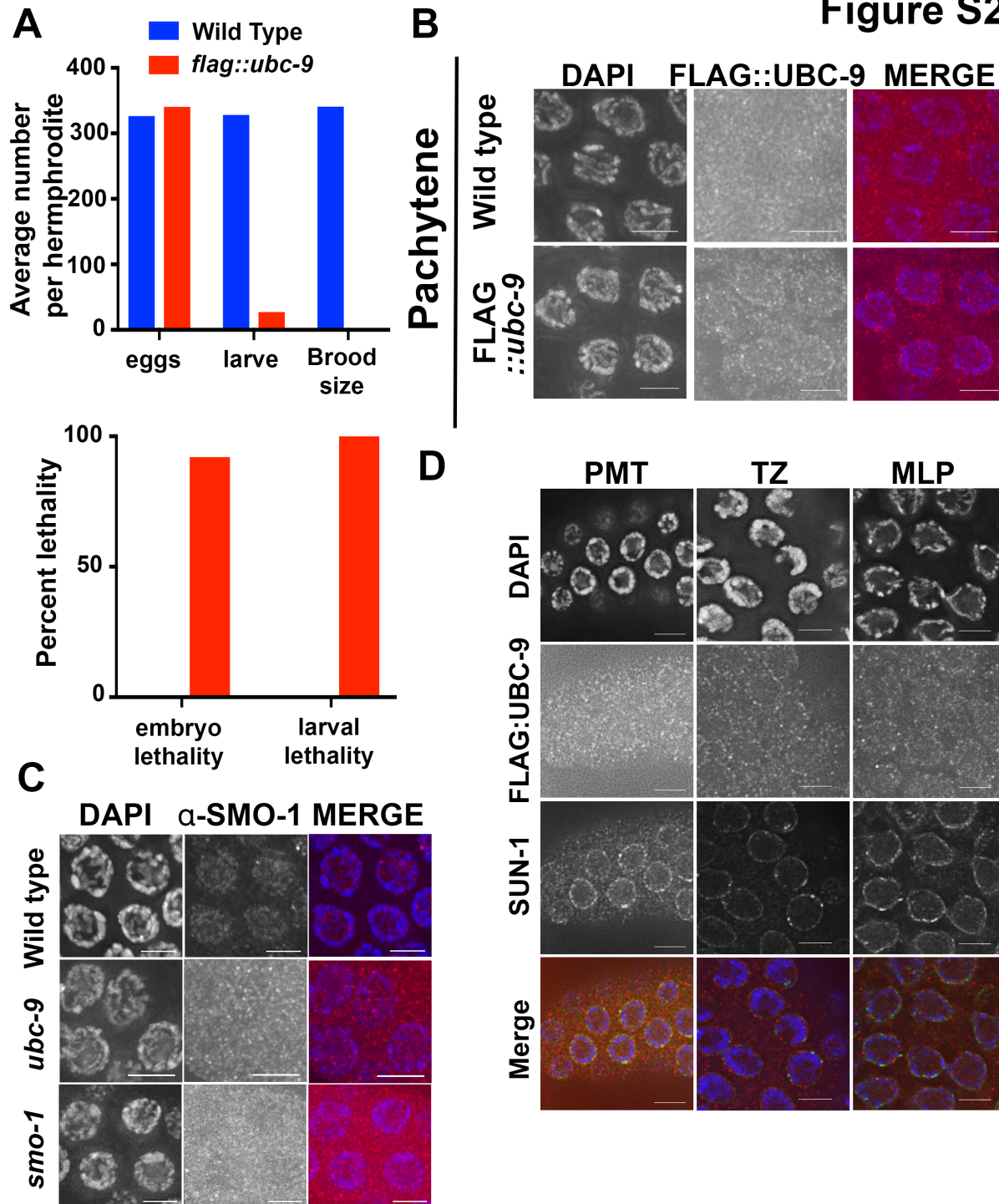
Supplemental Figure 1: *C. elegans* MRE-11 and UBC-9 interact via the yeast-two-hybrid assay.

A) X-gal interaction assay results between MRE-11 fused to the LexA DNA binding domain (DB) and UBC-9 fused to the LexA activating domain (AD). Full length MRE-11 as well as MRE-11 broken into two fragments (N-terminal half and C-terminal half with 100bp of overlap) were used verify interaction with UBC-9. Transformations of AD::UBC-9 and

DB::MRE-11 (N,C, and FL) are negative controls. B) List of plasmids present in yeast shown in

A.

Figure S2

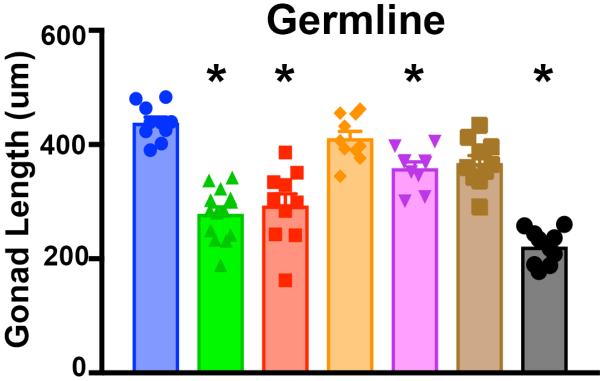


Supplemental Figure 2: SUMOylation protein localization in the germline. A) Fecundity assays were used to assess the *flag::ubc-9* homozygous line. There is normal egg-laying, but

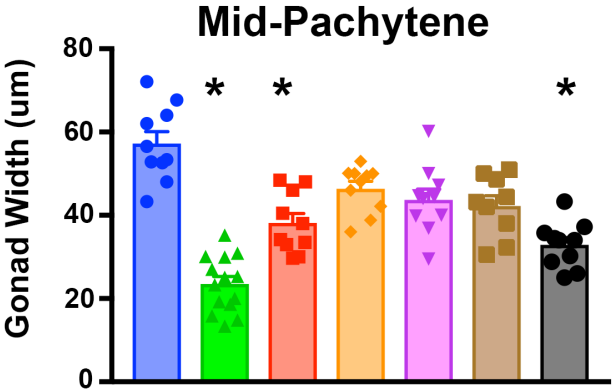
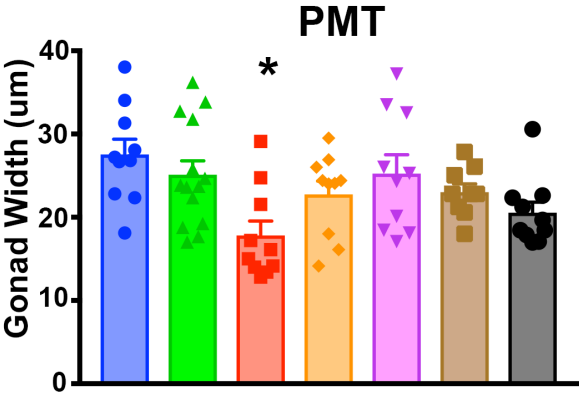
developmental issues prevent homozygotes from reaching adulthood. (Blue = WT, Red = *flag::ubc9* homozygotes) B) FLAG::UBC-9 localizes to the nuclear periphery in pachytene but not in the WT background. C) SMO-1 localizes to the nucleus in wild type, but not *ubc-9* or *smo-1* mutants in pachytene. D) 3XFLAG::UBC-9 and SUN-1 colocalize the germline. 3XFLAG::UBC-9 and SUN-1 images were taken in the pre-meiotic tip, transition zone, and mid/late pachytene. Colocalization is enhanced in the TZ and MLP.

A

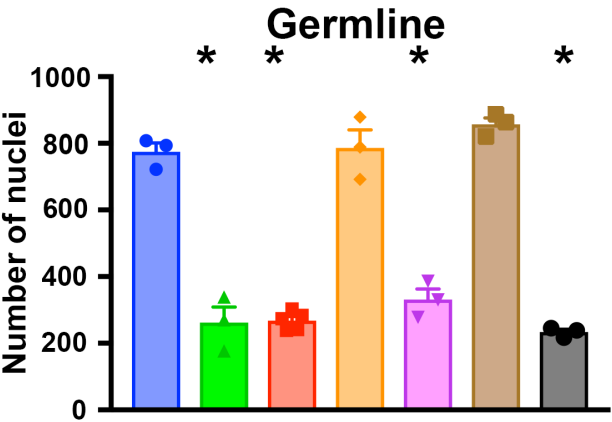
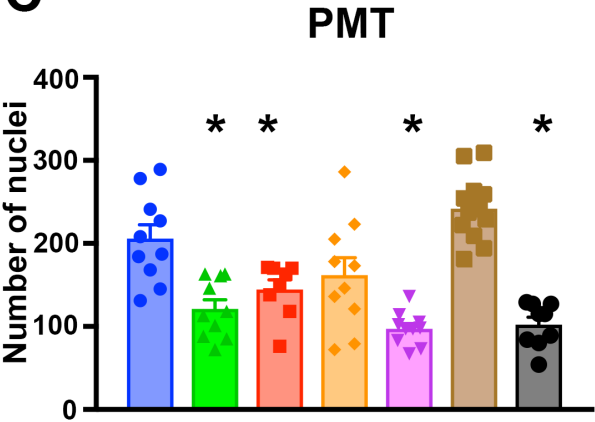
- Wild type
- ▲ *smo-1(ok359)*
- *ubc-9(tm2610)*
- ◆ *mre-11(iow1)*
- ▼ *ubc-9(tm2610); mre-11(iow1)*
- *spo-11(ok79)*
- *ubc-9(tm2610); spo-11(ok79)*



B

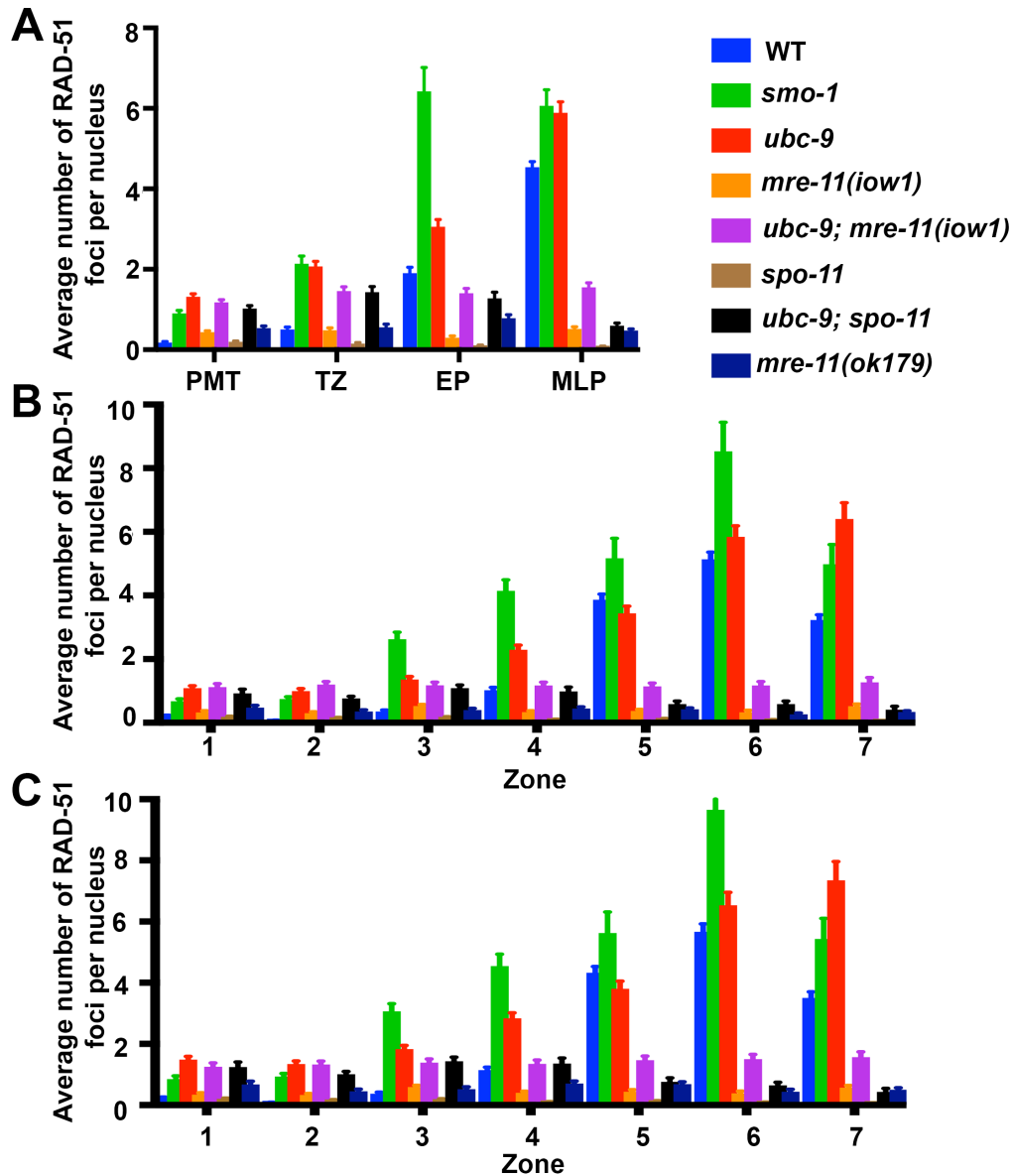


C

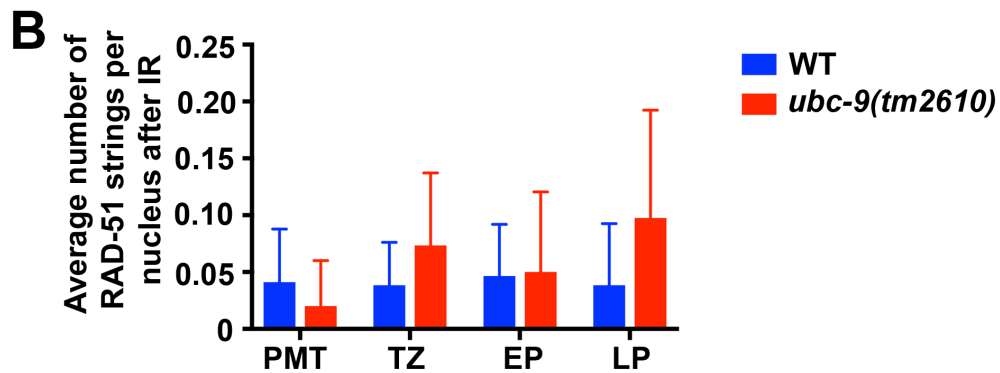
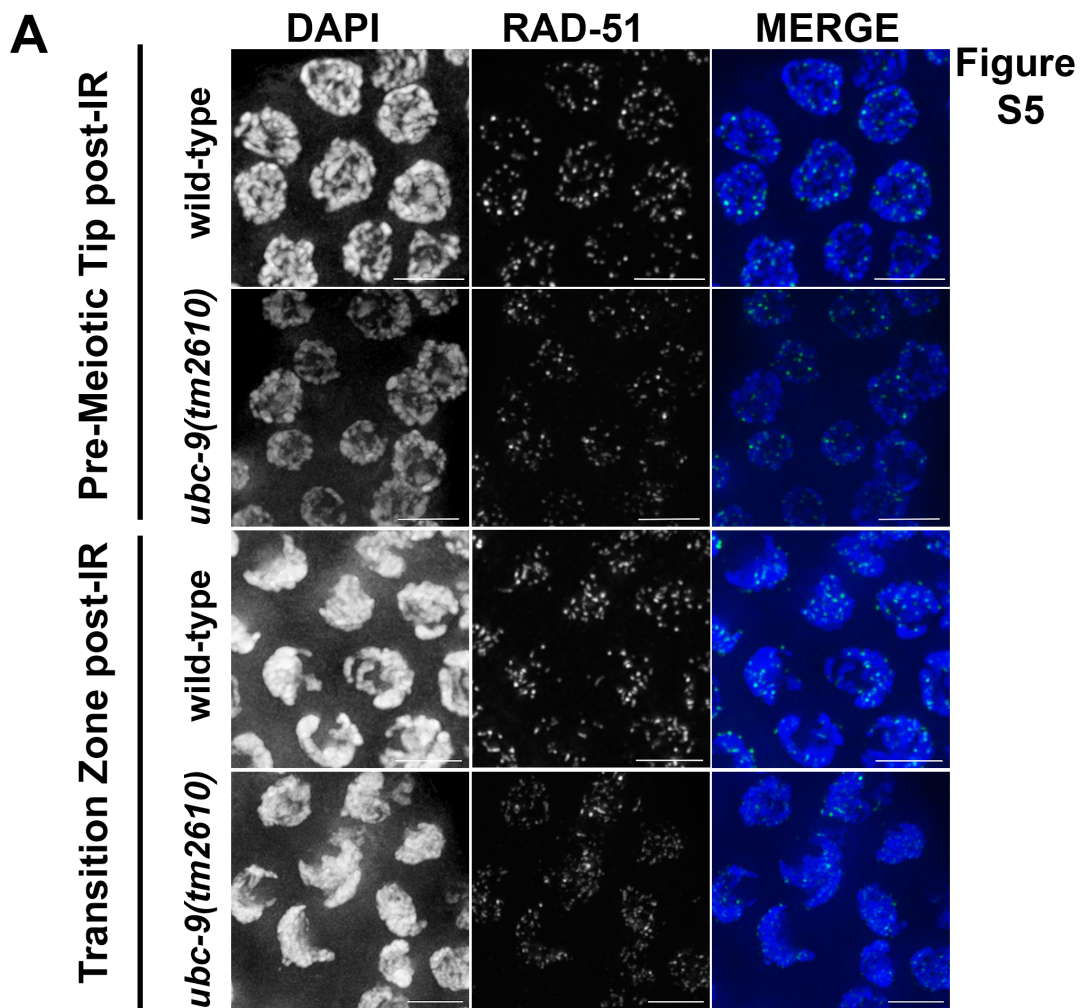


Supplemental Figure3: SUMOylation mutants have reduced numbers of nuclei and smaller gonads compared to wild type. A) Gonad length was measured from DAPI stained whole worms. Length was measured from the PMT to the end of pachytene/beginning of diplotene in ImageJ. At least 10 gonads were measured per genotype. B) Gonad width was measured at two

points during prophase I. PMT width was measured at a point 50% of the distance between the proximal tip of the PMT and the first discernable polarized nuclei indicating the beginning of the TZ. Length was measured in ImageJ. Mid-pachytene width was measured at the halfway point from the start of TZ to start of diplotene. Length was measured in ImageJ. At least 10 gonads were measured per genotype. C) Total number of nuclei in the PMT and whole gonad were counted from at least ten and three gonads per genotype, respectively. All asterisks indicate significance of $p < 0.05$ and all mutants are compared to wild type. Points on the graph indicate individual data points, with the bar indicating the mean of all data points. Error bars signify the mean \pm SEM.



Supplemental Figure 4: Alternative method of counting RAD-51 data. A) RAD-51 data counting aberrant foci as follows: singlets: 1, doublets: 2, triplets: 3, quadruplets: 4, strings: 1. Overall averages are increased, but the trends remain similar to Figure 2. Pairwise comparison can be found in supplemental data tables B-C) The same RAD-51 data presented above, except broken into zones as previously defined in (Yin and Smolikove). B) Clustered data (all types of RAD-51 foci counted as 1). C) Data counted as in A above. Error bars signify the mean \pm SEM.



Supplemental Figure 5: RAD-51 strings are not increased after irradiation of *ubc-*

9(tm2610) worms. A) WT and *ubc-9(tm2610)* strains were irradiated for five minutes at 10Gy.

Worms were dissected, fixed and stained for RAD-51 and strings counted. B) Because of the

overall increase in RAD-51 foci, doublet/triplet/quadruplet formations could not be measured, but strings could be identified. Error bars signify the mean \pm SEM.